IBRO Neuroscience Reports 10 (2021) 96–103

Contents lists available at ScienceDirect

IBRO Neuroscience Reports

journal homepage: www.sciencedirect.com/journal/IBRO-Neuroscience-Reports

Research Paper

Analysis of morphological and neurochemical changes in subthalamic nucleus neurons in response to a unilateral 6-OHDA lesion of the substantia nigra in adult rats

Katayoun Sedaghat [1], Andrew L. Gundlach, David I. Finkelstein [*]

The Florey Institute of Neuroscience and Mental Health, The University of Melbourne, Victoria, Australia

ARTICLE INFO

Keywords:
Parafascicular nucleus
Parkinson's disease
Substantia nigra pars compacta (SNpc)
Subthalamic nucleus
Tyrosine hydroxylase (TH)
Vesicular glutamate transporter-2 (vGlut2)
6-Hydroxydopamine (6-OHDA) lesion

ABSTRACT

Background: Subthalamic nucleus (STN) neurons undergo changes in their pattern of activity and morphology during the clinical course of Parkinson's disease (PD). Striatal dopamine depletion and hyperactivity of neurons in the parafascicular nucleus (Pf) of the intralaminar thalamus are predicted to contribute to the STN changes.
Objective: This study investigated possible morphological and neurochemical changes in STN neurons in a rat model of unilateral, nigral dopamine neuron loss, in relation to previously documented alterations in Pf neurons.
Methods: Male Sprague-Dawley rats received a unilateral injection of 6-hydroxydopamine (6-OHDA) into the substantia nigra pars compacta (SNpc). Rats were randomly divided into two groups (6/group) for study at 1 and 5 months by post-treatment. The extent of SNpc dopamine neuron damage was assessed in an amphetamine-induced rotation test and postmortem assessment of tyrosine hydroxylase mRNA levels using in situ hybridization histochemistry. Neural cross-sectional measurements and assessment of vesicular glutamate transporter-2 (vGlut2) mRNA levels were performed to measure the impact on neurons in the STN.
Results: A unilateral SNpc dopaminergic neuron lesion significantly decreased the cross-sectional area of STN neurons ipsilateral to the lesion, at 1 month ($P < 0.05$) and 5 months ($P < 0.01$) post-lesion, while bilateral vGlut2 mRNA levels in STN neurons were unaltered.
Conclusions: Decreased size of STN neurons in the presence of sustained vGlut2 mRNA levels following a unilateral SNpc 6-OHDA lesion, indicate altered STN physiology. This study presents further details of changes within the STN, coincident with observed alterations in Pf neurons and behaviour.
Data availability: The data associated with the findings of this study are available from the corresponding author upon request.

1. Introduction

The basal ganglia are composed of a number of subcortical nuclei, which are involved in the control of motor function, and their dysfunction is implicated in Parkinson's disease (PD). The subthalamic nucleus, (STN), is a part of the basal ganglia and is a glutamatergic nucleus that sends most of its projections to globus pallidus interior and exterior and substantia nigra pars reticulata (SNpr). Its activity is mainly regulated by inhibitory GABAergic projections from globus pallidus and glutamatergic fibers from cortex and intralaminar thalamus. It also receives scattered dopaminergic fibers from SNpc projections that pass the STN dorsally (Rommelfanger and Wichmann, 2010). Animal models of PD revealed that the activity of the STN is altered within the first few weeks after a dopaminergic lesion of the SNpc (Orieux et al., 2000; Henderson et al., 2005; Aymerich et al., 2006; Degos et al., 2013; Wang et al., 2013). This increase in activity is at least partly due to alterations in the activity of the projections to the STN from an intralaminar thalamic nucleus, known as the parafascicular nucleus (Pf) or centromedian-parafascicular (CM-Pf) nucleus (Smith et al., 2014; Parker et al., 2016). The Pf receives projections from the SNpr and it has been reported that a significant decrease in the dopaminergic innervation of the thalamic CM-Pf might be the underlying reason for clinical manifestations such as deficits in verbal fluency and attention, disturbances in sleep (Monje et al., 2020). The Pf sends motor and non-motor

* Corresponding author.
E-mail address: david.finkelstein@florey.edu.au (D.I. Finkelstein).
[1] Current address: Department of Physiology, School of Medicine, Semnan University of Medical Sciences, Semnan, Iran

https://doi.org/10.1016/j.ibneur.2021.01.002
Received 12 October 2020; Received in revised form 28 December 2020; Accepted 12 January 2021
Available online 3 February 2021

projections to several basal ganglia structures in rodents, including caudate putamen (CPu), STN, SNpr and the entopeduncular nucleus (Krout et al., 2002; Tsumori et al., 2002; Galvan et al., 2015). In rats with a unilateral excitotoxic Pf lesion, apomorphine administration causes ipsilateral rotation towards the lesion side, indicating the close interaction of Pf with basal ganglia structures. Glutamatergic Pf neurons project to striatal median spiny neurons (MSNs) and interneurons and interacts with striatal dopamine and acetylcholine systems (Kilpatrick and Phillipson, 1986; Consolo et al., 1996; Ferre et al., 2007).

Previous studies have demonstrated that Pf neurons undergo neurodegeneration in PD. Neuropathological data have shown a significant neurodegeneration restricted to the CM-Pf in humans (Henderson et al., 2000), primates (Lanciego et al., 2009) and rodents (Aymerich et al., 2006). One study suggests that the degeneration in Pf in PD, is a primary event and not a consequence of degeneration in the SN (Kusnoor et al., 2012). However, not all the neurons in the Pf degenerate, a population of neurons not only survive, but appear to be over-activated, with an increase in metabolic rate and size (Aymerich et al., 2006). In fact, Pf neurons that project to the STN in rats do not degenerate after nigrostriatal denervation and exhibit hyperactivity and increase the excitation of the STN (Orieux et al., 2000). Studies of changes in the thalamo-striatal neuronal pathway, reflected by vesicular glutamate transporter-2 (vGlut2) and cyclooxygenase 1 (COX-1), mRNA levels, revealed substantially increased metabolic activity and changes in the firing rate of Pf and STN neurons, following a partial SNpc lesion (Aymerich et al., 2006). Indeed, there has been an expanded scientific interest in STN function due to the common use of STN stimulation as a therapy for PD (Antonini and Obeso, 2018; Fox et al., 2018).

The time course of the morphological and functional changes in Pf neurons indicates that most of the changes are limited to the initial stages of the 6-OHDA model of PD and alterations do not continue throughout the course of this model of the disease (Sedaghat et al., 2009). Earlier we reported that a population of Pf neurons increased their activity after a unilateral dopaminergic lesion of the SNpc in adult male rats, with a likely peak increase at ~1 month, after which these neurons gradually regain their normal activity (Sedaghat et al., 2009). Therefore, the aim of this study was to further investigate these animals to determine any possible changes in the morphology, including size, and neurochemical activity of STN neurons, one and five months after a unilateral 6-OHDA lesion of the SNpc.

2. Materials and methods

2.1. Animals

Male Sprague-Dawley rats, weighing 200–300 g, were obtained from the Animal Resource Centre (Perth, WA, Australia). Rats were housed 2 per cage under a 12-h light/dark cycle and were given access to standard rat chow and water ad libitum. Animal care was conducted in accordance with the National Health and Medical Research Council of Australia guidelines on the care and use of animals in research. These experiments were approved by the Florey Institute of Neuroscience and Mental Health Animal Ethics Committee. The work described in this manuscript have been carried out in accordance with the Code of Ethics of the World Medical Association, EC Directive 86/609/EEC for animal experiments. All efforts were made to minimize the number of animals used and their suffering.

2.2. Unilateral 6-OHDA lesion of substantia nigra pars compacta

A 6-OHDA lesion was induced unilaterally as described (Sedaghat et al., 2009). Briefly, rats were anaesthetized with a mixture of ketamine hydrochloride (28 mg/kg, i.p.) and xylazine (2.4 mg/kg, i.p.). 6-OHDA (Sigma-Aldrich, Castle Hill, NSW, Australia) was injected at two different sites according to a rat brain atlas (Paxinos and Watson, 2007), at the following stereotaxic co-ordinates: AP 3.7 mm, ML − 1.7 mm, DL 8.1 mm (first injection) and AP 3.7 mm, ML − 2.1 mm, DL 7.5 mm (second injection) using a 23-gauge injection needle (0.63 mm OD, SGE, Ringwood, VIC, Australia) connected via single lumen polyethylene tube (OD 1.00 mm × ID 0.5 mm) to a 100 µl Hamilton syringe (SGE), mounted on a syringe pump (Cole-Palmer; Extech Equipment, Vernon Hills, Illinois, USA). A concentration of 2.5 µg/µl of 6-OHDA diluted in 0.2% ascorbic acid was infused at a rate of 1 µl/min (2 µl injection volume) to produce a ≥ 70% cell loss in the SNpc (Stanic et al., 2003; Sedaghat et al., 2009). For five days after the surgery, rats were monitored and weighed and then maintained under normal housing conditions for the duration of the experiment.

The effectiveness of the lesion was assessed in each rat two weeks after the 6-OHDA treatment as described (Sedaghat et al., 2009) by testing for rotation asymmetry following an amphetamine HCl injection (5 mg/kg i.p., Sigma-Aldrich). In brief, before testing, rats were placed in a plastic bin for 30 min for acclimatization, during which their behaviour was recorded. After amphetamine injection their behaviour was recorded for a further 60 min. The average number of turns per min (net number of turns (right minus left) made in 140 min) for pre- and post-amphetamine injection were compared. Rats were then allocated to groups (n = 6) that were kept for 1 or 5 months, before being sacrificed with an overdose of anaesthetic and processed for further analysis. While we did not generate groups of sham-operated rats, a group of naïve, unoperated rats were kept under identical conditions for 1 (3 rats) or 5 (3 rats) months and were processed as age-matched controls with the 1- and 5-month post-lesion groups. After anaesthetic overdose rats were decapitated and their brains were removed, frozen over liquid nitrogen, and stored at –80 °C for later processing.

2.3. In situ hybridization histochemistry for vGlut2 and TH mRNA

The in situ hybridization histochemistry (ISHH) protocol for determining the levels of tyrosine hydroxylase (TH), and vGlut2 mRNA was as described (Sedaghat et al., 2009). Briefly, adjacent or near-adjacent coronal sections (14 µm) from control and 6-OHDA lesioned brains (collected at the level of the STN, rostrocaudally; (−3.60) to (−5.20) mm relative to bregma) were delipidated and incubated with specific [^{35}S]-labeled oligonucleotide probes for vGlut2 mRNA (Table 1). Coronal sections at the level of the SNpc were delipidated and incubated with [^{35}S]-labeled oligonucleotides for tyrosine hydroxylase (TH) mRNA (Table 2). Oligonucleotides were labeled with [α-^{35}S]-dATP (Amersham Radiochemical Centre, UK) using terminal deoxynucleotide transferase (TdT) in a buffer containing co-factors and $CoCl_2$. Labeled probe was diluted in minimum hybridization buffer containing 100% formamide, 20 × SSC (Standard Saline Citrate: 3 M NaCl, 0.3 M tri-sodium citrate, pH 7.0) and 10% dextran sulphate. Slide-mounted sections were incubated with hybridization buffer at 42 °C overnight and then slides were washed in the 1 × SSC at 55 °C for 60 min, rinsed and dehydrated with ethanol and exposed to Kodak Biomax film (Integrated Sciences, Sydney, NSW, Australia) for 10 days. Slides were subsequently dipped in Ilford K5 emulsion (Ilford Imaging, Melbourne, VIC, Australia) allowed to dry and then stored in the dark at 4 °C for approximately 15 days, prior to development. Following development, sections were counterstained with 0.01% thionin and coverslipped for analysis using bright- and dark-field microscopy. Digital images from

Table 1
Sequences of oligonucleotide probes used to detect rat vGlut-2 mRNA.

Probe	Nucleotides	Oligonucleotide Sequence (5–3′)
rvGlut2–1	55–93	ACA GAT TGC ACT TGA TGG GAC TCT CAC GGT CTG TTT TGA
rvGlut2–2	1353–1391	CTC CCA GCC GTT AGG CCA GCC TCC GTT CTC CTG TGA GGT
rvGlut2–3	2000–2038	TGT CTA ACG TGA ACT ACC CTG AGA GTG CCA GAC AAA ACT

Source – NCBI, Accession number NW_047558.2.

Table 2
Sequences of oligonucleotide probes used to detect rat TH mRNA.

Probe	Nucleotides	Oligonucleotide Sequence (5–3′)
rTH-1	1329–1367	ACA GCT CAT GGC AGC AGT CCG GCT CAG GTG AAT GCA TAG
rTH-2	1625–1663	GTA CAC AGG CTG GTA GGT TTG ATC TTG GTA GGG CTG CAC

Source – NCBI, Accession number NM_012740.2.

X-ray films were obtained using MCID software with a Sony XC-77 monochrome camera and Northern Lights light box. Brightfield photomicrographs of nuclear emulsion-dipped counterstained sections were produced using an Olympus BX51 photomicroscope and a Microfire camera (Optronics Inc., Goleta, California, USA).

2.4. Quantitative analysis of the vGlut2 mRNA levels and neuronal size of STN neurons

A quantitative assessment of the density of vGlut2 mRNA in STN neurons following unilateral, 6-OHDA lesions of SNpc was conducted by analysing neuronal size and the number of silver grains associated with cellular labeling produced by [^{35}S]-oligonucleotide probes in nuclear-emulsion autoradiograms, using *Image J* software (NIH, Bethesda, MD, USA, Version 1.37). These measurements were performed on brain sections from the 1- and 5-month post-lesion groups and the time-matched, naïve control groups. Data was collected from the STN in both hemispheres, representing the ipsilateral and contralateral side of the STN, relative to the side containing the unilateral 6-OHDA lesion. For data collection, the STN was divided to three zones, dorsal, medial and ventral (Fig. 1).

2.5. Statistical analysis

Statistical analysis of the different data sets was performed using one-way and two-way ANOVA followed by Sidak's post-test for pairwise comparison of data for control and lesioned brains (ipsilateral and contralateral to lesion), using GraphPad, Prism software (version 8.00, GraphPad Software, La Jolla, CA, USA) and for Chi-square functions, Minitab Release (version 14.2 USA 2005). Data was graphed using GraphPad, Prism 8.00 software.

3. Results

3.1. Characterization of unilateral 6-OHDA lesion of SNpc

The relative effectiveness of the 6-OHDA lesion on the nigrostriatal dopaminergic pathway in each rat was assessed 14 days after surgery using an amphetamine-induced rotation test. Subsequently, the regional confinement of the lesion to the SNpc and the extent of dopamine neuron loss, were confirmed postmortem in the 1- month and 5-month survival groups, using thionin staining and ISHH (Sedaghat et al., 2009). The rotational asymmetry tests demonstrated that after amphetamine injection (5 mg/kg, i.p.), rats with the 6-OHDA lesion increased their number of rotations from a baseline of 0.13 ± 0.01 rotations to 7.40 ± 0.81 turns/min (n = 12, paired *t*-test; $P < 0.001$), in line with previous studies (Stanic et al., 2003; Sedaghat et al., 2009). The extent of the lesion in all rats included in the subsequent analysis from the 1- and 5-month groups was confirmed by a clear reduction in TH mRNA on the lesioned side compared to the unlesioned side of the midbrain (Fig. 2 A, B).

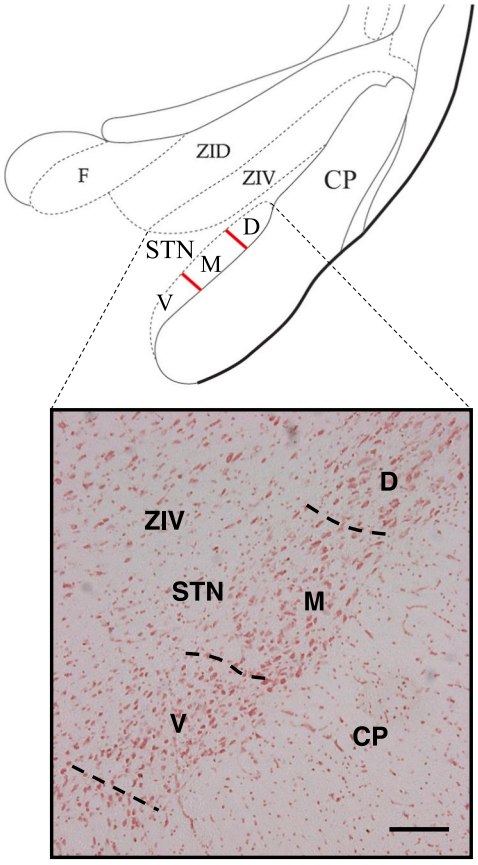

Fig. 1. Schematic diagram and photomicrograph of a Nissl-stained section of the subthalamic nucleus of the rat (at a coronal level of −4.2 mm from bregma), indicating the three regions in which the morphological analysis was performed (solid and dotted lines). Abbreviations: CP, cerebral peduncle; F, fornix; STN (D/M/V), subthalamic nucleus (dorsal/medial/ventral); ZI (D/V), zona incerta (dorsal/ventral). Scale bar, 300 μm.

3.2. vGlut2 mRNA in STN neurons 1- and 5-months after unilateral 6-OHDA SNpc lesion

A two-way ANOVA of the relative density of vGlut2 mRNA-associated silver grains detected on the ipsilateral and contralateral side to the lesion relative to control, indicated that the expression of vGlut2 mRNA in the STN was not significantly different between the ipsi- and contralateral sides ($F_{(1,76)} = 0.556$, $P = 0.458$) or between the 1- and 5-month groups ($F_{(1,76)} = 0.054$, $P = 0.816$). The relative level of vGlut2 mRNA as a percentage of control for the ipsilateral side to the lesion at 1-month and 5-months post-lesion was 93.22 ± 13.57% and 87.26 ± 13.47% of control, respectively, and for the contralateral side was 100.8 ± 23.81% and 100.4 ± 15.84% of control, respectively (mean ± SEM, n = 3–5 rats per group, density of silver grains per cell (grains/μm^2); Fig. 3).

3.3. Morphology of STN neurons at 1- and 5-months after unilateral 6-OHDA SNpc lesion

A two-way ANOVA revealed a significant difference between the cross-sectional area of neurons across the STN ipsilateral and contralateral to the 6-OHDA lesion and those in the control group ($F_{(2117)} = 7.468$, $P = 0.0009$); but no difference between the cross-sectional area of STN neurons in the 1- and 5-month post-lesion groups and no significant interactions for side post-lesion (ipsi- or contra-lateral) or control × time (Fig. 4). Sidak's multiple comparison test revealed a highly significant difference between the neuronal cross-sectional area

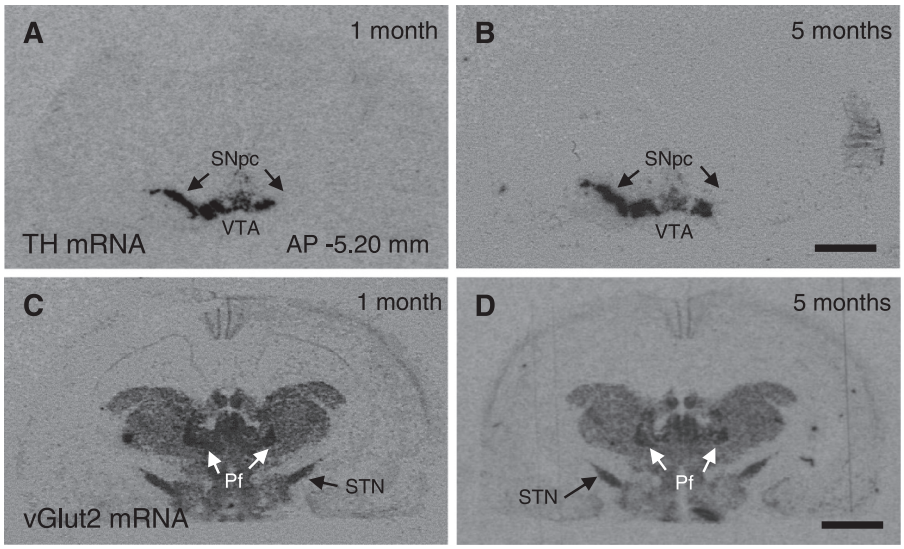

Fig. 2. (A, B) Representative X-ray film autoradiograms of tyrosine hydroxylase (TH) mRNA detected in the midbrain at the level of the SNpc and ventral tegmental area (VTA; approx. −5.20 mm from bregma), 1- and 5-months after a unilateral 6-OHDA lesion of the SNpc. Arrows indicate the normal levels and total loss of TH mRNA associated with the SNpc on the contralateral and ipsilateral sides, respectively. (C, D) Representative X-ray film autoradiograms of vesicular glutamate transporter (vGlut2) mRNA detected in the thalamus at the level of the STN and Pf (approx. −4.16 mm from bregma), 1- and 5-months after a unilateral 6-OHDA lesion, respectively. Scale bars, 2.5 mm.

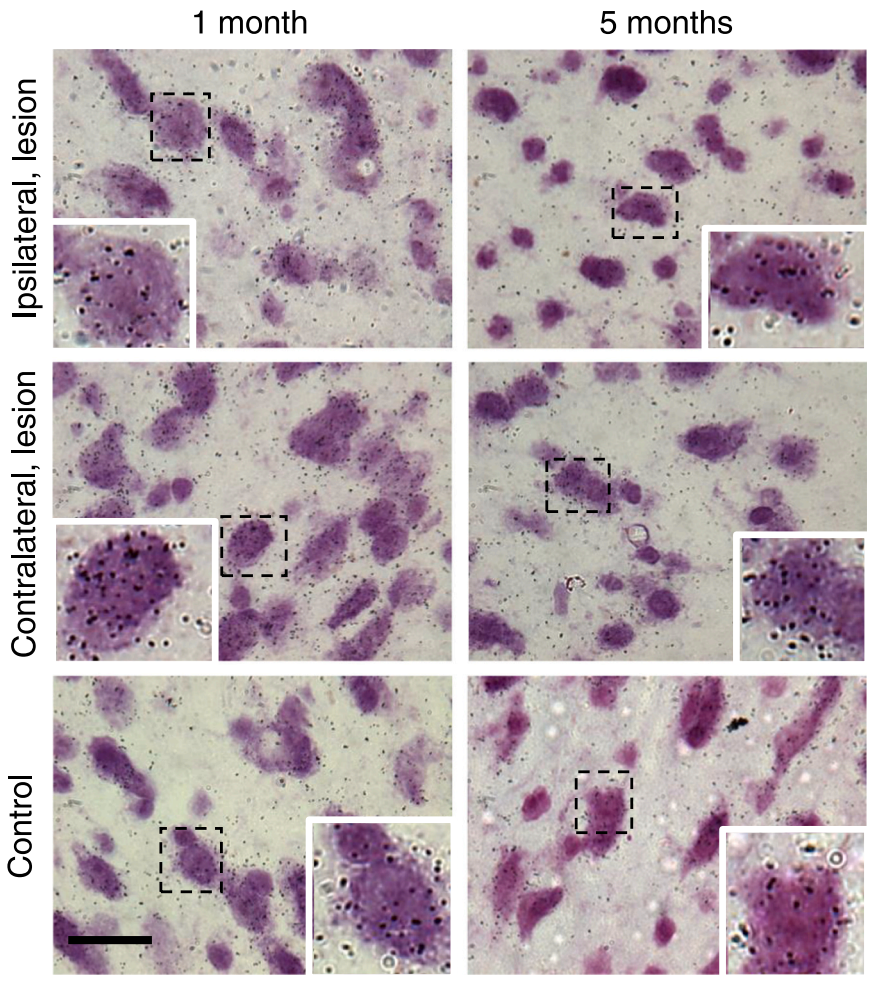

Fig. 3. Photomicrographs of Nissl-stained, nuclear-emulsion autoradiograms illustrating vGlut2 mRNA-associated silver grains over neurons in the dorsomedial STN from the ipsilateral and contralateral side of rats with a unilateral 6-OHDA lesion of SNpc and time-matched control rats 1-month (left column) and 5-months (right column) post-lesion/survival time. Insets illustrate exemplary cells and their associated quantity of silver grains, as indicated by a dashed box on each panel. The relative density of vGlut2 mRNA-associated silver grains was similar in all groups (data not shown). Scale bar is 10 micron.

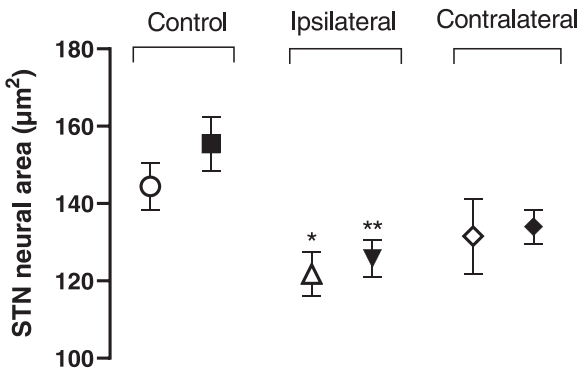

Fig. 4. Cross-sectional area (μm^2) of STN neurons from ipsilateral (n = 40) and contralateral (n = 40) sides to the SNpc lesion and from control brains (n = 40), 1-month (open circle, triangle, and diamond symbols) and 5-months (black square, triangle and diamond symbols) after 6-OHDA lesion. Two-way ANOVA indicated that the cross-sectional area of STN neurons on the ipsilateral side to the 6-OHDA lesion was smaller than STN cells in control rats at 1-month (*P < 0.05) and 5-months (**P < 0.01) post-lesion. The cross-sectional area of STN neurons on the contralateral side to the 6-OHDA lesion was not significantly different to that of STN neurons in control rats at 1-month (P = 0.4192) and 5-months (P = 0.063).

of STN neurons in control rats and those ipsilateral to the lesion at 5 months (P = 0.0046), and a more moderate difference at 1 month post-lesion (P = 0.0443), suggesting that the cross-sectional area of STN neurons is reduced between 1- and 5-months post-lesion. Across the STN on the contralateral side to the 6-OHDA lesion, despite a numerical decrease in the mean cell cross-sectional area, the reduction was not significantly different from control (Fig. 4).

3.4. Regional comparison of STN neurons after unilateral 6-OHDA SNpc lesion

A comparison of the cross-sectional area of neurons in the three STN regions (dorsal, medial and ventral) on the lesioned and contralateral sides of the 6-OHDA-treated (1- and 5-month survival) rats, relative to those in age-matched control rats revealed that neurons in the dorsal and medial STN ipsilateral and contralateral to the SNpc lesion had significantly smaller cross-sectional areas than those in the ventral region. A 2-way ANOVA of STN neurons on the ipsilateral side to the 6-OHDA SNpc lesion identified a marked size difference between the dorsal, medial and ventral regions ($F_{(2,74)} = 4.272$, P = 0.0176), no difference between the time post-lesion, and a significant difference for regions × time post-lesion ($F_{(2,74)} = 3.701$, P < 0.05). Sidak's multiple comparison test revealed a significant difference between the 5-month dorsal and ventral STN regions (P = 0.0037, Figs. 5 and 6A). For STN

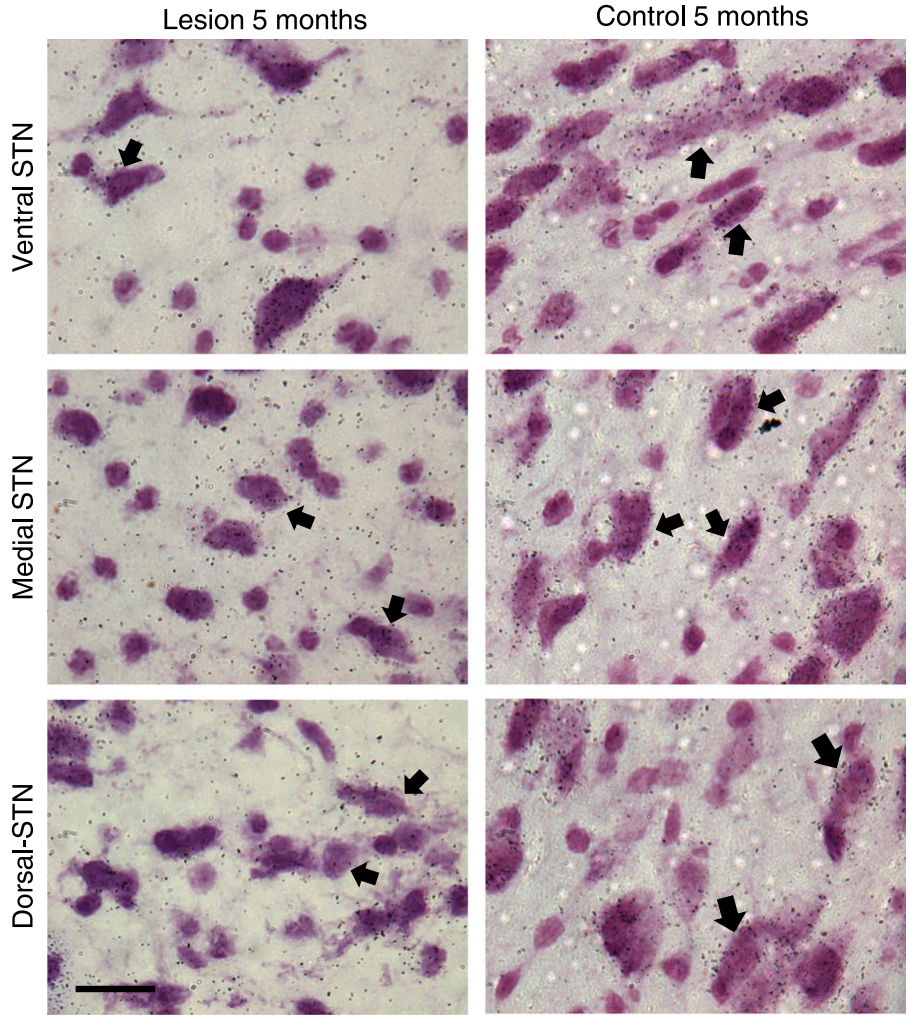

Fig. 5. Photomicrographs of Nissl-stained sections (nuclear-emulsion autoradiograms) illustrating the dorsal, medial and ventral regions of the STN ipsilateral to the 6-OHDA SNpc lesion 5-months after treatment and of the STN of an age-matched, control rat. In the STN ipsilateral to the 6-OHDA SNpc lesion, round-shaped cells are abundant (arrows), while in the STN of control brain, spindle-shaped cells are more prevalent (arrows). Scale bar 10 micron.

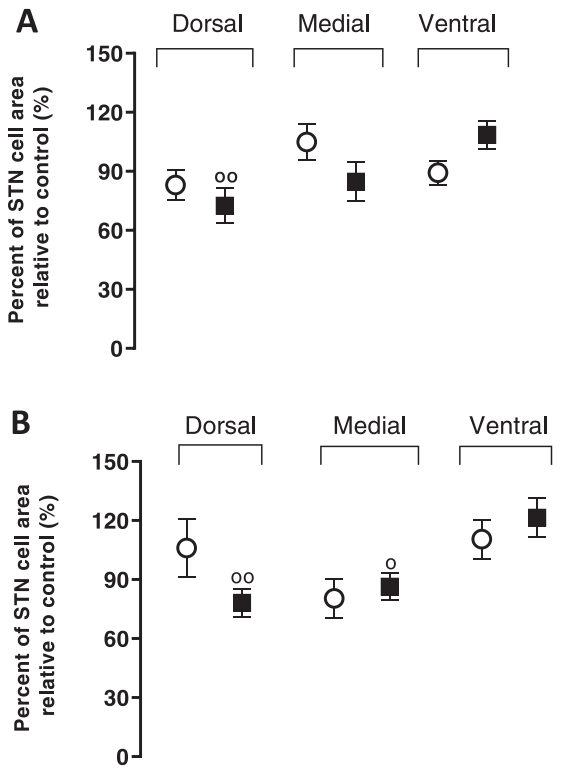

Fig. 6. (A) Comparison of neuronal cross-sectional area in the dorsal, medial and ventral regions of STN ipsilateral to the 6-OHDA SNpc lesion, relative to those in equivalent control rats at 1- and 5-months (open circle and black square, respectively). Two-way ANOVA revealed a significant difference between the dorsal and ventral STN at 5-months post-lesion (**P < 0.01). (B) Comparison of neuronal cross-sectional area in the dorsal, medial and ventral regions of STN contralateral to the 6-OHDA SNpc lesion, relative to those in equivalent control rats at 1- and 5-months (open circle and black square, respectively). Two-way ANOVA revealed a significant difference between neuronal areas in the dorsal and medial STN, and the ventral STN, at 5-months post-lesion (**P < 0.01 and *P < 0.05, respectively).

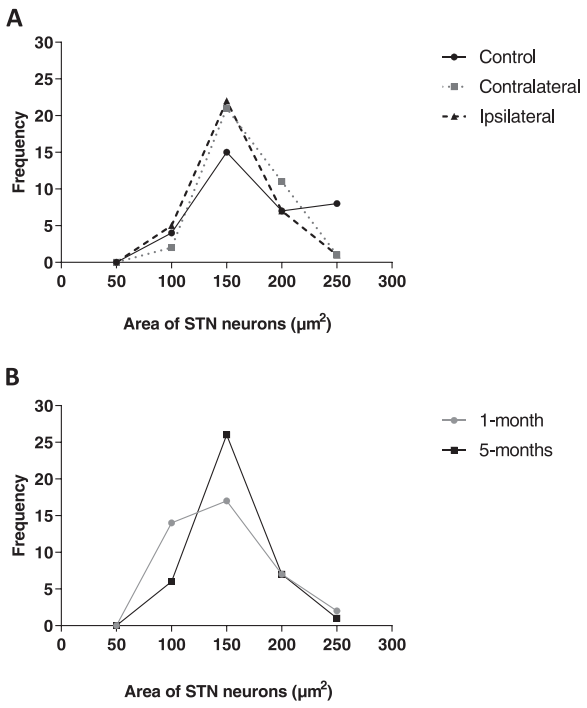

Fig. 7. (A) Frequency distribution of cell areas of vGlut2 mRNA-positive cells in the STN of control rats and the ipsilateral and contralateral sides of 6-OHDA SNpc lesioned rats at 5-months post-lesion. The peak frequency for STN cell area in the control and ipsilateral to lesion groups is 150 μm^2, but the frequency distribution of cells with an area < 150 μm^2 was significantly higher than control (Chi-square, P < 0.05, n = 35). (B) Frequency distribution of cell areas for vGlut2 mRNA-positive cells ipsilateral to the 6-OHDA SNpc lesion at 1- and 5-months post-lesion. The peak frequency for STN cell area in both groups is 150 μm^2. The frequency curve of STN cells 1-month post-lesion is shifted to the left (indicating smaller cells) relative to the 5-month group, but this difference is not significant (Chi-square, P = 0.07, n = 40).

neurons on the contralateral side to the 6-OHDA SNpc lesion, a marked difference was identified between dorsal, medial and ventral regions ($F_{(2,74)} = 6.100$, P = 0.0035). Sidak's multiple comparison test revealed a significant difference between medial and ventral (P = 0.0463) and dorsal and ventral regions (P = 0.0068) 5-months post-lesion (Figs. 5 and 6B). Therefore, after a unilateral 6-OHDA lesion of SNpc, it appears that only the dorsal and medial regions of STN are affected, while the ventral region remains unaffected.

The frequency distribution of the cross-sectional area of STN neurons ipsilateral to the 6-OHDA SNpc lesion at 1-month post-lesion, and in control rats, demonstrated a trend for a shift in the size frequency of ipsilateral neurons towards smaller cell sizes, but this shift was not significant relative to control (data not shown). In the 5-month post-lesion group, although the peak frequency of the control STN neurons and those ipsilateral to the lesion was 150 μm^2, a significantly higher number of STN cells ipsilateral to the lesion, displayed a cross-sectional area of 150 μm^2 relative to control (Chi-square, P < 0.05, Fig. 7).

4. Discussion

In this study of a hemi-Parkinsonian model involving a unilateral 6-OHDA lesion of the SNpc in adult male rats, we observed morphological changes in dorsal and medial STN neurons, reflected by a decrease in the cross-sectional area, both ipsilateral and contralateral to the SNpc lesion at 5-months post-lesion. Concurrently, the metabolic activity of the STN neurons, reflected by the neuronal density of vGlut2 mRNA (Aymerich et al., 2006) was not different between the 1- and 5-months post-lesion and age-and time-matched control groups.

The small alteration in the cross-sectional area of STN neurons observed at 1-month post-lesion was somewhat in contrast to previous studies which reported initial hyperactivity of STN neurons, reflected by increased expression of vGlut2 and COX-1 mRNA (Hirsch et al., 2000; Breit et al., 2001; Aymerich et al., 2006; Jouve et al., 2010). Furthermore, an earlier study reported that after a unilateral SNpc lesion, the firing rate of STN neurons was increased slightly 1 day after the lesion, peaked after 7 days, and was ~190% of control at 14 days (Hirsch et al., 2000). In other studies the activity of the STN and Pf nuclei was assessed at various times, including 7 (Mouroux et al., 1995) and 8 days (Hassani et al., 1996), and 2 (Aymerich et al., 2006) and 3 weeks (Hassani et al., 1996; Breit et al., 2001), after nigral lesion. However, in most of these studies, any hyperactivation of the STN had subsided by 2 weeks after the lesion. The comparable levels of vGlut2 mRNA detected at 1- and 5-months after the lesion, may suggest any initial increase in the activity of STN neurons ipsilateral to the nigral lesion may have been transient and was not captured by the survival times in this study.

Many previous studies have demonstrated that after dopamine denervation, cortico-striatal projections produce hyperactivity within basal ganglia (Favier et al., 2013). In addition to the motor cortex, it is known that another likely driver of STN hyperactivity in the first weeks after nigral dopaminergic neuron lesions is hyperactivity of Pf neurons (Orieux et al., 2000), and hyper-stimulation by Pf projections, in addition to increased activation by cortical projections, might be excitotoxic

for STN neurons (Henderson et al., 2000; Blum et al., 2001; Hilker et al., 2005). Therefore, the observed reduction in the neuronal cross-sectional area of STN neurons, particularly at 5 months after the nigral lesion, might be explained by toxicity of STN neurons. A compensatory adjustment in vGlut2 mRNA levels may have occurred, as we did not observe any difference in the cellular density of vGlut2 mRNA in STN neurons in the 5-month group compared to the 1-month post-lesion and the control groups. Therefore, our data suggest the reported hyperactivity of STN neurons immediately subsequent to the nigral lesion is a transient effect and is eventually replaced by a persistent alteration in STN neuron size and function, which persists for much longer after the nigral lesion.

We also observed a reduction in the cross-sectional area of neurons in the dorsal STN on the contralateral side to the nigra lesion. Notably, neuronal tract-tracing studies reveal that the Pf sends afferents to the STN in both hemispheres (Marini et al., 1999; Castle et al., 2005). If the Pf has bilateral projections to the STN and is hyperactivated in unilateral rat PD models, this might cause changes in the contralateral as well as the ipsilateral STN.

In the morphological analysis of the STN, we divided the nucleus into dorsal, medial and ventral regions. The STN has distinct functional zones in the human brain (Lambert et al., 2012), so we divided the rat STN into three anatomical regions to approximate these functional areas. Previous studies in primates have also considered the segregation of STN zones on the basis of cortical inputs, which identified clearer subdivisions that observed in rodent STN. In rats, the dorsolateral and dorsomedial areas of the STN mainly receive projections from motor cortex (M1and M2), while the medial area receives most of its inputs from orbital and limbic areas of cortex such as cingulate, frontal prelimbic, infralimbic and lateral orbital cortices (Janssen et al., 2010; Kita et al., 2014). The output from rat STN to the cerebral cortex is mostly to the orofacial motor area, sensorimotor and prefrontal areas, while the well-known STN output to basal ganglia is to the ipsilateral SNpr, entopeduncular nucleus and the external segment of the globus pallidus (Degos et al., 2008).

Regarding thalamo-subthalamic projections, they enter the nucleus via the ventral region. Different regions of the Pf send projections to all three STN regions, e.g., dorsolateral and medial Pf sends fibres to dorsal and medial STN (Groenewegen and Berendse, 1990; Kita et al., 2016). Following a unilateral SNpc lesion, neurons in the ventromedial and dorsolateral Pf undergo degeneration and the remaining neurons display increased activity (Sedaghat et al., 2009), which is consistent with findings in the current study that neurons in the medial and dorsal STN displayed decreased cross-sectional area at 5-months post-lesion. Projections from cortex and intralaminar nuclei innervate the dorsolateral and medial subdivisions of STN, which are the sites where the decrease in neural cross-sectional area was observed in the current study, and the site of outputs that eventually terminate in motor and prefrontal cortices. Therefore these anatomical changes could be the origin of motor, cognitive and motivational disturbances (Ferrazzoli et al., 2018) produced in animal models of PD or even in human sufferers.

A comparison of the shape of STN neurons in the three regions in the 5-month post-lesion and control groups revealed that on the ipsilateral side to the lesion, most neurons were round in shape, while in the age-matched controls, neurons were oval or fusiform in shape, suggesting that healthy oval-shaped neurons may be impacted by the lesion, resulting in either degeneration or altered morphology. Notably, previous studies have described the morphology of STN cells in different species, and fusiform or spindle-shaped cells are widely reported in different species including rodents (Kita et al., 1983; Pearson et al., 1985; Marani et al., 2008; Emmi et al., 2020). Since several studies have identified oval or spindle neurons as the main outputs of STN, the decline of such cells observed in our study may reflect degeneration of specific outputs of STN to globus pallidus and SNpr in the hemi-Parkinsonian model in rat.

5. Conclusion

In this study we observed that 1-month following unilateral lesion of SNpc with 6-OHDA no marked changes occurred in vGlut2 mRNA expression and only minor changes occurred in the cross-sectional area of STN neurons. However, 5-months after the SNpc dopaminergic lesion, we observed altered morphology and a clear reduction in the neuronal cross-sectional area of dorsal and medial STN neurons, ipsi- and contralateral to the nigral lesion, compared to neurons in intact control rats, suggesting reduced activity and possible excitotoxicity in the STN. Since, the density of vGlut2 mRNA (grains per μm^2) did not change, despite a reduction in the cell cross-sectional area; it is likely that by 5-months after the nigral lesion, the production of vGlut2 mRNA is also reduced. The decrease in neural activity within the STN 5-months after the nigral lesion may be the result of toxicity produced by hyperactivation of projections from the Pf to STN during the initial period (1–2 weeks) after the 6-OHDA lesion of SNpc. Finally, this study of a hemi-Parkinsonian model of PD demonstrated that the morphology of neurons was differentially altered in different anatomical regions of the STN, consistent with the patterns of activity change and neurodegeneration in the Pf after a unilateral SNpc lesion (Sedaghat et al., 2009).

CRediT authorship contribution statement

Katayoun Sedaghat: Conceptualization, Data curation, Formal analysis, Investigation, Methodology, Validation, Visualization, Writing - original draft and editing. **Andrew L. Gundlach**: Conceptualization, Formal analysis, Funding acquisition, Methodology, Project administration, Resources, Supervision, Validation, Visualization, Writing - review and editing. **David I. Finkelstein**: Conceptualization, Formal analysis, Investigation, Methodology, Project administration, Resources, Software, Supervision, Validation, Visualization, Writing - review and editing.

Acknowledgments

The authors would like to thank Doris Tomas for her assistance with the 6-OHDA lesions.

Role of the funding source

This research was supported by a project grant from the National Health and Medical Research Council (NHMRC) of Australia (1005988, ALG) and a grant from the Brain Foundation Australia (ALG). The funding sources had no involvement in the study design; in the collection, analysis and interpretation of data; in the writing of the report; or the decision to submit the article for publication.

Conflict of interest

The authors have no conflict of interest to report.

References

Antonini, A., Obeso, J.A., 2018. DBS for Parkinson's disease with behavioural disturbances. Lancet Neurol. 17, 195–197. https://doi.org/10.1016/S1474-4422(18)30044-9.

Aymerich, M.S., Barroso-Chinea, P., Perez-Manso, M., Munoz-Patino, A.M., Moreno-Igoa, M., Gonzalez-Hernandez, T., Lanciego, J.L., 2006. Consequences of unilateral nigrostriatal denervation on the thalamostriatal pathway in rats. Eur. J. Neurosci. 23, 2099–2108. https://doi.org/10.1111/j.1460-9568.2006.04741.x.

Blum, D., Torch, S., Lambeng, N., Nissou, M., Benabid, A.L., Sadoul, R., Verna, J.M., 2001. Molecular pathways involved in the neurotoxicity of 6-OHDA, dopamine and MPTP: contribution to the apoptotic theory in Parkinson's disease. Prog. Neurobiol. 65, 135–172.

Breit, S., Bouali-Benazzouz, R., Benabid, A.L., Benazzouz, A., 2001. Unilateral lesion of the nigrostriatal pathway induces an increase of neuronal activity of the

pedunculopontine nucleus, which is reversed by the lesion of the subthalamic nucleus in the rat. Eur. J. Neurosci. 14, 1833–1842.
Castle, M., Aymerich, M.S., Sanchez-Escobar, C., Gonzalo, N., Obeso, J.A., Lanciego, J.L., 2005. Thalamic innervation of the direct and indirect basal ganglia pathways in the rat: Ipsi- and contralateral projections. J. Comp. Neurol. 483, 143–153.
Consolo, S., Baronio, P., Guidi, G., Di Chiara, G., 1996. Role of the parafascicular thalamic nucleus and N-methyl-D-aspartate transmission in the D1-dependent control of in vivo acetylcholine release in rat striatum. Neuroscience. 71, 157–165.
Degos, B., Deniau, J.M., Chavez, M., Maurice, N., 2013. Subthalamic nucleus high-frequency stimulation restores altered electrophysiological properties of cortical neurons in Parkinsonian rat. PLoS One 8, e83608. http://e8360810.1371/journal.pone.0083608.
Degos, B., Deniau, J.M., Le Cam, J., Mailly, P., Maurice, N., 2008. Evidence for a direct subthalamo-cortical loop circuit in the rat. Eur. J. Neurosci. 27, 2599–2610. https://doi.org/10.1111/j.1460-9568.2008.06229.x.
Emmi, A., Antonini, A., Macchi, V., Porzionato, A., De Caro, R., 2020. Anatomy and connectivity of the subthalamic nucleus in humans and non-human primates. Front Neuroanat. 14, 13 https://doi.org/10.3389/fnana.2020.00013.
Favier, M., Carcenac, C., Drui, G., Boulet, S., El Mestikawy, S., Savasta, M., 2013. High-frequency stimulation of the subthalamic nucleus modifies the expression of vesicular glutamate transporters in basal ganglia in a rat model of Parkinson's disease. BMC Neurosci. 14, 152. https://doi.org/10.1186/1471-2202-14-152.
Ferrazzoli, D., Ortelli, P., Madeo, G., Giladi, N., Petzinger, G.M., Frazzitta, G., 2018. Basal ganglia and beyond: the interplay between motor and cognitive aspects in Parkinson's disease rehabilitation. Neurosci. Biobehav. Rev. 90, 294–308. https://doi.org/10.1016/j.neubiorev.2018.05.007.
Ferre, S., Agnati, L.F., Ciruela, F., Lluis, C., Woods, A.S., Fuxe, K., Franco, R., 2007. Neurotransmitter receptor heteromers and their integrative role in 'local modules': the striatal spine module. Brain Res. Rev. 55, 55–67.
Fox, S.H., Katzenschlager, R., Lim, S.Y., Barton, B., de Bie, R.M.A., Seppi, K., Coelho, M., Sampaio, C., Movement Disorder Society Evidence-Based Medicine, C., 2018. International Parkinson and movement disorder society evidence-based medicine review: update on treatments for the motor symptoms of Parkinson's disease. Mov. Disord. 33, 1248–1266. https://doi.org/10.1002/mds.27372.
Galvan, A., Devergnas, A., Wichmann, T., 2015. Alterations in neuronal activity in basal ganglia-thalamocortical circuits in the parkinsonian state. Front Neuroanat. 9, 5. https://doi.org/10.3389/fnana.2015.00005.
Groenewegen, H.J., Berendse, H.W., 1990. Connections of the subthalamic nucleus with ventral striatopallidal parts of the basal ganglia in the rat. J. Comp. Neurol. 294, 607–622. https://doi.org/10.1002/cne.902940408.
Hassani, O.K., Mouroux, M., Feger, J., 1996. Increased subthalamic neuronal activity after nigral dopaminergic lesion independent of disinhibition via the globus pallidus. Neuroscience 72, 105–115.
Henderson, J.M., Carpenter, K., Cartwright, H., Halliday, G.M., 2000. Degeneration of the centre median-parafascicular complex in Parkinson's disease. Ann. Neurol. 47, 345–352.
Henderson, J.M., Schleimer, S.B., Allbutt, H., Dabholkar, V., Abela, D., Jovic, J., Quinlivan, M., 2005. Behavioural effects of parafascicular thalamic lesions in an animal model of parkinsonism. Behav. Brain Res. 162, 222–232. https://doi.org/10.1016/j.bbr.2005.03.017.
Hilker, R., Portman, A.T., Voges, J., Staal, M.J., Burghaus, L., van Laar, T., Koulousakis, A., Maguire, R.P., Pruim, J., de Jong, B.M., Herholz, K., Sturm, V., Heiss, W.D., Leenders, K.L., 2005. Disease progression continues in patients with advanced Parkinson's disease and effective subthalamic nucleus stimulation. J. Neurol. Neurosurg. Psychiatry 76, 1217–1221.
Hirsch, E.C., Perier, C., Orieux, G., Francois, C., Feger, J., Yelnik, J., Vila, M., Levy, R., Tolosa, E.S., Marin, C., Trinidad Herrero, M., Obeso, J.A., Agid, Y., 2000. Metabolic effects of nigrostriatal denervation in basal ganglia. Trends Neurosci. 23 (Suppl), S78–S85.
Janssen, M., Visser-Vandervalle, V., Temel, Y., 2010. Cortico-subthalamic projections in the rat. J. Expl. Clin. Med. 27, 4–11.
Jouve, L., Salin, P., Melon, C., Kerkerian-Le Goff, L., 2010. Deep brain stimulation of the center median-parafascicular complex of the thalamus has efficient anti-parkinsonian action associated with widespread cellular responses in the basal ganglia network in a rat model of Parkinson's disease. J. Neurosci. 30, 9919–9928. https://doi.org/10.1523/JNEUROSCI.1404-10.2010.
Kilpatrick, I.C., Phillipson, O.T., 1986. Thalamic control of dopaminergic functions in the caudate-putamen of the rat I. the influence of electrical stimulation of the parafascicular nucleus on dopamine utilization. Neuroscience. 19 (3), 965–978.
Kita, H., Chang, H.T., Kitai, S.T., 1983. The morphology of intracellularly labeled rat subthalamic neurons: a light microscopic analysis. J. Comp. Neurol. 215, 245–257. https://doi.org/10.1002/cne.902150302.
Kita, T., Osten, P., Kita, H., 2014. Rat subthalamic nucleus and zona incerta share extensively overlapped representations of cortical functional territories. J. Comp. Neurol. 522, 4043–4056. https://doi.org/10.1002/cne.23655.
Kita, T., Shigematsu, N., Kita, H., 2016. Intralaminar and tectal projections to the subthalamus in the rat. Eur. J. Neurosci. 44, 2899–2908. https://doi.org/10.1111/ejn.13413.
Krout, K.E., Belzer, R.E., Loewy, A.D., 2002. Brainstem projections to midline and intralaminar thalamic nuclei of the rat. J. Comp. Neurol. 448, 53–101.
Kusnoor, S.V., Bubser, M., Deutch, A.Y., 2012. The effects of nigrostriatal dopamine depletion on the thalamic parafascicular nucleus. Brain Res. 1446, 46–55. https://doi.org/10.1016/j.brainres.2012.01.040.
Lambert, C., Zrinzo, L., Nagy, Z., Lutti, A., Hariz, M., Foltynie, T., Draganski, B., Ashburner, J., Frackowiak, R., 2012. Confirmation of functional zones within the human subthalamic nucleus: patterns of connectivity and sub-parcellation using diffusion weighted imaging. Neuroimage 60, 83–94. https://doi.org/10.1016/j.neuroimage.2011.11.082.
Lanciego, J.L., Lopez, I.P., Rico, A.J., Aymerich, M.S., Perez-Manso, M., Conte, L., Combarro, C., Roda, E., Molina, C., Gonzalo, N., Castle, M., Tunon, T., Erro, E., Barroso-Chinea, P., 2009. The search for a role of the caudal intralaminar nuclei in the pathophysiology of Parkinson's disease. Brain Res. Bull. 78, 55–59. https://doi.org/10.1016/j.brainresbull.2008.08.008.
Marani, E., Heida, T., Lakke, E., Usunoff, K.G., 2008. The subthalamic nucleus: Part I: development, cytology, topography and connections. Adv. Anat. Embryol. Cell Biol. 198, 1–113.
Marini, G., Pianca, L., Tredici, G., 1999. Descending projections arising from the parafascicular nucleus in rats: trajectory of fibers, projection pattern and mapping of terminations. Somatosens Mot Res. 16, 207–222.
Monje, M.H.G., Blesa, J., Garcia-Cabezas, M.A., Obeso, J.A., Cavada, C., 2020. Changes in thalamic dopamine innervation in a progressive Parkinson's disease model in monkeys. Mov. Disord. 35, 419–430. https://doi.org/10.1002/mds.27921.
Mouroux, M., Hassani, O.K., Feger, J., 1995. Electrophysiological study of the excitatory parafascicular projection to the subthalamic nucleus and evidence for ipsi- and contralateral controls. Neuroscience 67, 399–407.
Orieux, G., Francois, C., Feger, J., Yelnik, J., Vila, M., Ruberg, M., Agid, Y., Hirsch, E.C., 2000. Metabolic activity of excitatory parafascicular and pedunculopontine inputs to the subthalamic nucleus in a rat model of Parkinson's disease. Neuroscience 97, 79–88. https://doi.org/10.1016/S0306-4522(00)00011-7.
Parker, K.L., Kim, Y., Alberico, S.L., Emmons, E.B., Narayanan, N.S., 2016. Optogenetic approaches to evaluate striatal function in animal models of Parkinson disease. Dialogues Clin. Neurosci. 18, 99–107.
Paxinos, G., Watson, C., 2007. The Rat Brain in Stereotaxic Coordinates. Academic Press Australia, Australia.
Pearson, J.C., Norris, J.R., Phelps, C.H., 1985. Subclassification of neurons in the subthalamic nucleus of the lesser bushbaby (Galago senegalensis): a quantitative Golgi study using principal components analysis. J. Comp. Neurol. 238, 323–339. https://doi.org/10.1002/cne.902380307.
Rommelfanger, K.S., Wichmann, T., 2010. Extrastriatal dopaminergic circuits of the basal ganglia. Front Neuroanat. 4, 139 https://doi.org/10.3389/fnana.2010.00139.
Sedaghat, K., Finkelstein, D.I., Gundlach, A.L., 2009. Effect of unilateral lesion of the nigrostriatal dopamine pathway on survival and neurochemistry of parafascicular nucleus neurons in the rat – evaluation of time-course and LGR8 expression. Brain Res. 1271, 83–94. https://doi.org/10.1016/j.brainres.2009.03.026.
Smith, Y., Galvan, A., Ellender, T.J., Doig, N., Villalba, R.M., Huerta-Ocampo, I., Wichmann, T., Bolam, J.P., 2014. The thalamostriatal system in normal and diseased states. Front Syst. Neurosci. 8, 1–18. https://doi.org/10.3389/fnsys.2014.00005.
Stanic, D., Finkelstein, D.I., Bourke, D.W., Drago, J., Horne, M.K., 2003. Timecourse of striatal re-innervation following lesions of dopaminergic SNpc neurons of the rat. Eur. J. Neurosci. 18, 1175–1188. https://doi.org/10.1046/j.1460-9568.2003.02800.x.
Tsumori, T., Yokota, S., Ono, K., Yasui, Y., 2002. Synaptic organization of GABAergic projections from the substantia nigra pars reticulata and the reticular thalamic nucleus to the parafascicular thalamic nucleus in the rat. Brain Res. 957, 231–241.
Wang, Z., Myers, K.G., Guo, Y., Ocampo, M.A., Pang, R.D., Jakowec, M.W., Holschneider, D.P., 2013. Functional reorganization of motor and limbic circuits after exercise training in a rat model of bilateral parkinsonism. PLoS One 8, e80058. https://doi.org/10.1371/journal.pone.0080058.